Manipulation of defects on oxide surfaces via barrier reduction induced by atomic force microscope tips

Mathew B. Watkins and Alexander L. Shluger
Department of Physics and Astronomy, University College London, Gower Street, London WC1E 6BT, United Kingdom
(Received 23 December 2005; published 30 June 2006)

We used theoretical modeling to propose possible mechanisms of defect manipulation using a noncontact atomic force microscope (NC-AFM) on a generic oxide, MgO. First, we simulated NC-AFM images of a Ca substitutional defect on the MgO surface aiming to help identify a site where tip polarity could be reliably identified, and as a possible target for manipulation. We conclude that controlled manipulation of *substitutional* ions on the MgO surface is not feasible due to the strength of the interaction within the surface. Secondly, we demonstrate that controlled manipulation of a charged surface O vacancy can be easily achieved via the reduction of a vacancy diffusion barrier by the tip electrostatic potential, which facilitates thermal vacancy diffusion.

DOI: 10.1103/PhysRevB.73.245435 PACS number(s): 81.16.Ta, 61.72.Bb, 68.37.Ps, 68.47.Gh

I. INTRODUCTION

Scanning probe microscopes have revolutionized surface science by allowing direct real-space imaging of surfaces with atomic resolution. Further exploitation of these techniques leads naturally to attempting to use the microscopes to go beyond imaging and to directly influence the position or even the chemistry of specific sites on the surface, in a controlled manner. Atomic and molecular manipulation has been demonstrated repeatedly with scanning tunneling microscopy (STM), from relatively simple construction of ordered arrays of atoms through to inducing controlled reactions of molecules (see, for example, Refs. 1–3). However, STM is limited to conducting substrates. With an eventual aim of producing viable nanoscale electronic devices, manipulation on insulating materials will be needed. As a first cousin of STM, atomic force microscopy (AFM) is a potential tool for deployment, not being limited in the substrates it can operate on. However, manipulation of atoms and molecules with AFM carries considerable complexities that are not faced by the STM technique. Manipulation of atomic size species has only recently been observed with noncontact AFM (NC-AFM) on semiconductor surfaces,[4–7] but controlled, reproducible manipulation has yet to be achieved on insulating surfaces. Therefore, a strong effort to improve the technique and to make it applicable to controlling and manipulating a wide range of molecular processes at insulator surfaces continues. Part of this effort is the development of a theoretical model that allows understanding and predicting experimental images and manipulation conditions.[8,9]

In a recent paper,[9] we investigated the mechanisms of NC-AFM imaging of small (formate ion) and relatively big ($C_{52}H_{72}O_3$) molecules adsorbed on two oxide surfaces, MgO(100) and TiO_2(110), respectively, and discussed the possibility of their manipulation using NC-AFM. MgO is a prototype oxide with many applications as a substrate and in catalysis. The last two years have seen a lot of progress in NC-AFM imaging of the MgO(100) surface with atomic resolution (see Refs. 10 and 11). Point defects as well as extended defects have been observed in room-temperature experiments, however their chemical nature has not been determined.[10] NC-AFM manipulation of some (again not identified) defects on the CaF_2(111) surface has also been reported.[12] This makes studying the mechanisms of NC-AFM imaging and manipulation of defects at ionic surfaces particularly relevant. Previously[13] we discussed the mechanisms of NC-AFM contrast formation on the MgO(100) surface with polar[14] and Si dangling-bond tips[15] and reported an image of a prototype substitutional defect on the LiF surface.[14] We have also calculated a topographical image of a Cr^{3+} impurity ion on the MgO(100) surface and demonstrated that the interaction with a polar tip can affect the probabilities and energies of radiative transitions in this ion.[16] The aim of this paper is to demonstrate that using polar tips one can significantly reduce barriers for ion and vacancy diffusion at ionic surfaces such as MgO, and suggest a mechanism and protocols for manipulating vacancies at the MgO(100) surface.

Controlled AFM manipulation of specific atomic and molecular species at surfaces requires their identification in the image and determination of their position with respect to other surface species. In other words, one would like to make sure that this is the object one wants to manipulate and be able to establish its adsorption or incorporation site with respect to the surface atoms. To achieve that AFM is solely reliant on the short-range chemical forces between the tip apex and the target. Therefore, the exact chemical nature of the tip and its atomic structure are crucial. The nature of the tip will also have a significant impact on any attempt to use the AFM for manipulation. Occasionally conclusions about the nature of the nanotip can be made by comparison with theoretical images.[17,18] However, in many cases the nature of the tip cannot be determined just by imaging a pure surface of such systems as MgO and the even less symmetric TiO_2(110) because the high surface symmetry does not allow one to distinguish between different possible tip chemical terminations.[9,19] Often tips are contaminated by the surface material. As we have discussed in Refs. 14 and 20, imaging, e.g., the square surface lattice of MgO by a MgO (or any other oxide) tip carries an ambiguity due to an uncertain tip polarity. One of the ways forward is to use surface markers, such as adsorbed molecules or impurity ions, for tip identi-

fication. To this end, in this paper we first consider a substitutional Ca point defect on a MgO surface to examine the possibilities of using defects as markers to aid tip characterization.

Having discussed tip characterization, we then examine manipulation proper. We can imagine several targets for manipulation: adsorbates, adatoms, and defects in the substrate surface. Here we examine the manipulation of substitutional Ca ions and oxygen vacancies on the MgO surface. One vital point for our purposes is that the energy barriers for diffusion of these defects without tip influence are large; if this were not the case they would not have a sufficient lifetime at one site to identify and manipulate with the microscope. We consider successful manipulation events from the point of view of alterations to the potential energy surface caused by tip proximity. This appears to be a useful way to discuss the manipulation process and allows us to extend the discussion of our static calculations to real NC-AFM experiments. We also discuss the relevant energy scales for various processes and suggest criteria for successful manipulation.

The paper is organized as follows. In the next section, we briefly discuss the tip and surface models and methods used for calculating the tip-surface interaction and NC-AFM images. The results of our modeling of imaging and manipulation of Ca impurity on MgO surface are discussed in Sec. III and the mechanisms of oxygen vacancy manipulation in Sec. IV. Finally, we discuss the results of this study in Sec. V.

II. METHODS OF CALCULATION

In most types of NC-AFM setups, a cantilever oscillates with large amplitude near its resonance frequency, and is held in the attractive part of the interaction even at the closest tip-surface distance.[21–23] When the tip is approaching the surface, this interaction affects the cantilever oscillations, and the resulting frequency shift as a function of lateral tip position, averaged over many cantilever oscillations, can be determined. An image is created by scanning the surface in the *xy* plane, e.g., at constant cantilever amplitude and keeping the frequency shift constant by controlling the equilibrium position of the cantilever.[21–24] Other modes, such as "constant height,"[25] small oscillation amplitude,[11,21] and imaging in a repulsive mode,[11] are also used. For interpretation of these images, knowledge of the relationship between the tip-surface forces and the detected parameters of the cantilever oscillations is required. This issue has been treated in a number of publications.[14,24,26] In this paper we focus on calculating the tip-surface interactions and predicting their influence on imaging defect centers. We neglect the long-range electrostatic forces, which may be caused by surface charging, and capacitance forces. The macroscopic van der Waals forces are included when constructing simulated images.

A. Tip model

Most of the commercial cantilevers are microfabricated from silicon and are covered by a native oxide layer. This layer is thought to be removed in some experiments by sputtering with Ar^+ ions. However, the chemical structure and geometry of the very end of the tip are practically impossible to control. Therefore, any nanotip model can only be justified based on circumstantial evidence and on comparison of calculated images with experiment. One such evidence is a contact between tip and surface often occurring during scanning. As a result, one can expect some degree of tip contamination by surface ions. As has been discussed in the recent paper by Heyde *et al.*,[11] the metallic tip used in that work to image the MgO surface is possibly also covered by MgO forming a sort of a stable cluster. In our previous SFM modeling,[13,20] we often used a MgO cluster as a nanotip model (see Fig. 1). It is a generic model of a hard oxide tip, which has the important advantage that there are reliable interatomic potentials for the interaction between MgO and alkali halides and other oxides. In this paper, a 64-atom MgO cube has been used orientated with a ⟨111⟩ axis perpendicular to the surface plane. This tip has the advantage that the tip polarity can be reversed by rotating the tip by 180°. This serves our purpose for examining prototype manipulation scenarios on an insulator, giving us access to both repulsive and attractive manipulation regimes in a straightforward manner. As we will see below, the strength and spatial distribution of the tip electrostatic potential play an important role in manipulating surface ions. This potential is strong in the narrow vicinity of the MgO tip and is similar to that for the Si tip terminated by an adsorbed O ion.[15,27]

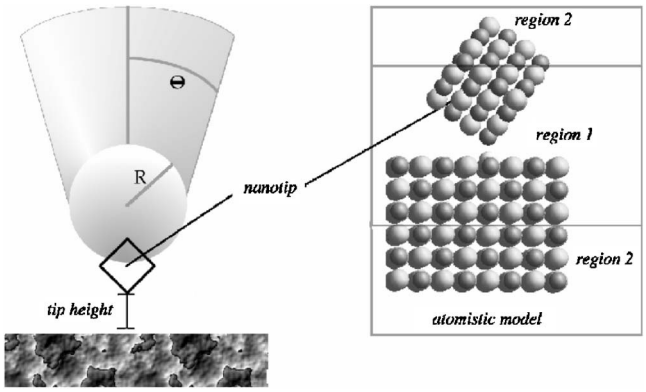

FIG. 1. Schematic of the setup used for modeling a NC-AFM experiment. The atomistic model used in manipulation calculations is shown in the magnified image on the right of the figure.

B. Computational details

In ultrahigh vacuum, the forces that are mostly responsible for the image contrast are determined by the "chemical" interactions between the tip apex and the surface atoms. To treat these interactions, we employ classical static atomistic techniques. The schematic model used in our calculations is shown in Fig. 1. The nanoasperity at the end of the tip and several upper surface layers are treated atomistically as described below.

We employed the atomistic simulation technique implemented in the GULP computer code, which is fully described in Refs. 28 and 29. The tip and surface ions were treated by the ionic model. Electronic polarization of ions is incorporated via the shell model,[30] in which an ion is considered to

consist of a core connected by a harmonic spring to a massless shell, i.e., the ion consists of two separate particles. The total charge of the ion is split between the core and shell. This partition and the harmonic spring constant determine the magnitude of the ionic polarization. All the ions in these calculations had their full formal charges and only polarization of the O^{2-} was taken into account. The parameters of the pair potentials for the interactions between ions inside MgO are described in Ref. 13. A recent investigation shows that these potentials give a good representation of the potential energy surface for all but complex cooperative ionic motions when compared to density-functional calculations.[31]

The nanotip and the upper surface layers are each split into two regions (I and II), as discussed in Refs. 13 and 20. The region I ions are relaxed explicitly until there is zero force on each of them, while those in region II are kept fixed to reproduce the potential of the bulk lattice and the rest of the tip on region I ions. The simulation cell shown in Fig. 1 has planar two-dimensional periodic boundary conditions parallel to the interface. To model a single tip at the surface, the interaction between the periodically translated nanotips and the interaction between the areas of surface deformation should be small. This is ensured by using a large surface area. When constructing images, the MgO surface region I contained three planes of 144 ions, which were allowed to relax. The surface region II contained three planes of frozen ions. For manipulation calculations, a smaller supercell with 64 ions per layer was used to allow us to efficiently explore the available phase space. Thirty-eight tip ions were allowed to fully relax to ensure that tip surface forces were fully accounted for; this is important as, especially when modeling manipulation, the tip approaches quite close to the surface.

III. IMAGING AND MANIPULATION OF Ca IMPURITY ON MgO SURFACE

MgO surface reveals the fundamental difficulty with tip characterization on highly symmetric oxide surfaces. When the MgO surface is imaged, the bright spots may be interpreted as a tip of positive polarity having a strong attractive interaction while positioned over the oxygen ions in the lattice. However, an equally likely explanation of the image is a negative polarity tip imaging the magnesium ions of the surface. In some situations it may be possible to break the surface symmetry if the tip induces strong surface relaxation, which has been discussed for CaF_2.[17] In general, though, it is necessary to break the symmetry by other means. This can be achieved by imaging adsorbates, if their absorption sites are known and they can be imaged with the necessary resolution at the same time as the substrate or, as we consider here, by examining point defects in the surface.

Experimental images of MgO (Ref. 10) usually reveal two main classes of defect. Larger objects, generally imaged as depressions, occupying areas from several atomic sites up to several nm^2, and smaller protrusions. The larger objects have been assigned to aggregates of vacancies in the surface created during the crystal cleavage and the surface preparation process; the smaller protrusions are of less certain provenance. Here we consider that the smaller objects may be Ca substitutional defects. Ca is known to be always present in MgO samples in significant concentrations. It tends to segregate to both MgO surface[32] and grain boundaries[33,34] as a result of high-temperature anneal. MgO samples can also be intentionally doped by Ca, and MgO/CaO solid solution films are known to be stable up to 500 °C.[35] Therefore, modeling of NC-AFM images of Ca ions at the surface may help their identification in experimental images. On the other hand, using MgO samples intentionally doped with Ca or other impurities can allow one to establish the tip polarity and hence to achieve chemical resolution of the surface ions.

A. NC-AFM images of Ca on MgO(100)

The larger ionic radii of the Ca ion compared to a Mg ion results in the Ca being pushed out of the surface by 0.3 Å; the neighboring O atoms also move approximately 0.1 Å in the positive z direction, in good agreement with the *ab initio* calculations of Ref. 36.

NC-AFM images of the Ca defect were calculated using the techniques described above, with tips of both polarities. The images are constructed in a constant frequency mode[20] using the following parameters: $A_{p-p}=5.7$ nm, $k=45$ N/m, $H=0.5518$ eV, $f_0=312$ KHz, $df=122$ Hz, and a tip radius of 23 nm, where A_{p-p} is the amplitude of the tip oscillations, k is the spring constant of the cantilever, H is the Hamaker constant, f_0 is the resonant frequency of the cantilever, and df is the average frequency detuning. These parameters are similar to published work that achieved atomic resolution on MgO (Ref. 10) and give a normalized frequency shift of 7.5 fN $m^{-1/2}$ that is typical for successful experimental measurements. Experimental images are usually constructed either in constant height mode, where a topographical image is formed by measuring the change in frequency shift of the cantilever as it is scanned over the surface, or in constant frequency shift mode (CFS), where a feedback loop is used to keep the frequency shift constant and an image is generated from the change in vertical position of the cantilever to maintain this constant shift. We first simulated the pure MgO surface, producing a corrugation of 30 pm in CFS mode in agreement with the results of Ref. 10.

In Fig. 2(a), we show a simulated image of the Ca defect with a negative polarity O tip. The Ca ion is imaged as a spherical protrusion, with a height almost 100 pm greater than that of Mg ions in the pure surface. The Ca ion's eight nearest neighbors cannot be separately resolved. Indeed the extent of the influence of the Ca ion extends out to next nearest neighbors in a (100) direction, where, despite being over 4 Å from the Ca, the force over a Mg ion is reduced by 0.3 eV/Å and the force curve is shifted to lower tip heights. This is attributed to interaction between the raised Ca and the Mg ions making up the second row of the nanotip. At the next nearest neighbor in a (110) direction, the convolution effects due to the Ca ion are virtually removed.

The positive polarity tip image of the Ca ion appears much as a reverse of the previous image [Fig. 2(b)]. The Ca ion appears as a depression of 100 pm, though the nearest-neighboring ions may be resolved in this case. Again it can be seen that next nearest neighbors in a (100) direction are

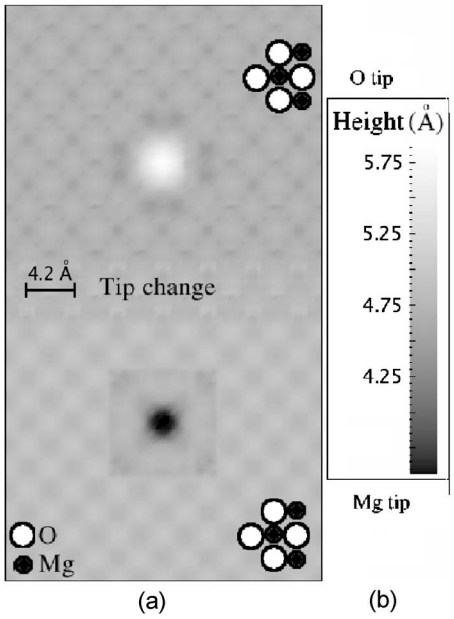

FIG. 2. Simulated NC-AFM images of a substitutional Ca impurity on MgO(001) with (top) O-terminated, negative polarity tip; (bottom) Mg-terminated, positive polarity tip. Parameters used to generate these images are given in the text.

seen to have a weaker interaction than those along a (110) direction.

These results provide some useful "fingerprints" for identifying Ca impurity ions on the MgO surface. They demonstrate that tip-defect convolution can affect NC-AFM images of even relatively simple substitutional surface defects. Recently, we discussed the importance of this effect for imaging a formate ion adsorbed on the MgO surface.[9] Finally, we note that our results demonstrate that impurities, such as Ca ions, should be clearly distinguishable on ionic surfaces and could serve as convenient indicators of the tip polarity before, after, and during imaging. This has also been demonstrated experimentally in the example of a mixed KCl:Br crystal in Ref. 37.

B. Manipulation of a substitutional defect

Manipulation of substitutional defects at semiconductor surfaces using NC-AFM has recently been reported.[4–7] To investigate the prospects on an ionic crystal, we have simulated several modes of manipulation of a Ca substitutional ion on the MgO surface. As discussed above, a Ca ion on a MgO(001) surface protrudes from the ideal surface by ~0.3 Å. We consider possible ways of forcing this ion to exchange sites with one of the nearest-neighbor surface Mg ions.

1. Attractive or pulling mode

We use the MgO cube tip with an O ion orientated as the apex atom. At the point of strongest attractive interaction, the Ca jumps into contact with the tip, moving a further 0.7 Å to be ~1.0 Å from the ideal surface. On retraction of the tip, the Ca ion jumps back into its original surface site. In terms of the potential energy surface, this means that as the tip retracts from the position where the Ca ion jumped into contact, there is little or no energy barrier to the Ca ion moving from the tip to the surface site, and that the surface site is considerably more stable. Furthermore, if instead of retracting the tip directly we also move it in a (110) direction, attempting to move the Ca ion laterally out of its site, we find that there is still an unfeasibly large energy barrier to be surmounted. Therefore, we conclude that a Ca ion cannot be easily manipulated out of its site to exchange with the Mg ion by the Coulomb attraction to the tip apex and investigate an alternative possibility of pushing it out of its site.

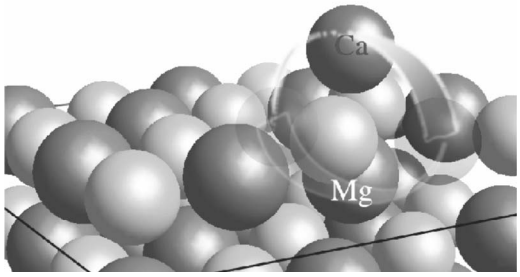

FIG. 3. Transition state for the exchange of a Ca impurity and a neighboring Mg ion.

2. Repulsive or pushing mode

We consider two operations, pushing the Ca atom into the surface causing it to interchange with a neighboring Mg ion, or pushing a neighboring Mg ion *mutatis mutandi*. As may be anticipated, pushing the larger Ca into the surface is less favorable and we focus on the second operation. This process is illustrated in Fig. 3. Without the tip present, we estimate the activation energy for this exchange process at 7.6 eV. This is due to the large Madelung potential of the MgO lattice containing doubly charged ions. We attempted to induce this reaction with a Mg terminated tip: The tip was placed at locations around and above the Mg ion we aim to move at tip heights between 1.5 and 3.0 Å. The most favorable location found was with the tip at a height of 2 Å, displaced 0.12 Å from above the surface Mg ion, away from the direction of induced motion. In this geometry, we can reduce the barrier to exchange by 4.0 eV. This is essentially caused by two factors: (i) destabilization of the initial geometry by the repulsive interaction between the Mg tip and the surface Mg atom, and (ii) an attractive interaction between an O atom on the second layer of the tip and the Ca ion as it is forced out of the surface by the motion of the Mg ion. However, the energy barrier is still far too large for any reaction to occur. Pushing harder, we observed two effects that prevented further barrier reduction.

(i) Damage to the tip: the apex Mg moves to the side of the tip and the three second-layer O ions form strong bonds to the surface

(ii) Motion of a neighboring O atom on the surface to the tip apex to prevent further destabilization of the system.

We conclude that in the case of an ionic crystal containing doubly charged ions, the potential energy loss for moving ions from their ideal location is too large for manipulation

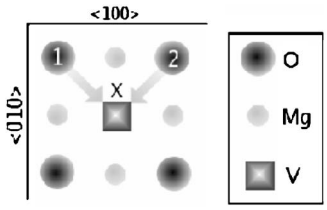

FIG. 4. Schematic of the vacancy diffusion process on MgO(001). Two oxygen ions that can be involved in manipulation are marked 1 and 2.

using even a very ionic AFM tip. We also note that the tip considered is about as strong as can easily conceived, however it is still softer than the surface and this limits the force that can be exerted in a repulsive pushing regime. On softer surfaces these conclusions will probably not hold, however we are always seeking a situation where the diffusion barrier of the target is far too large to permit thermal diffusion, which may hinder attempts at manipulation where energy barriers are smaller.

IV. MANIPULATION OF VACANCIES

It is known that ion diffusion in bulk MgO is vacancy-mediated. Therefore, as another prototype system we consider a doubly charged surface O vacancy. The importance of tip characterization is emphasized as we can manipulate the O vacancy with a tip of positive polarity, but find no corresponding mechanism for a negative polarity tip. (Note that as our tip is made of the same material as the surface, the interactions with a Mg vacancy are likely to be similar, but using an opposite polarity tip. We consider the more difficult motion, with the larger O anion moving.) There have been recent reports of the possible identification of an O vacancy on the MgO(001) surface and of manipulation of a Cl vacancy on KCl (Ref. 38) so these current calculations represent a system of current experimental interest.

A. Single O vacancy

The motion we intend to achieve is illustrated in Fig. 4, and corresponds to an O atom neighboring the vacancy moving in a (110) direction. Alternatively, this can be seen as the vacancy moving in the opposite direction. We find the diffusion barrier for the isolated O vacancy without the tip present to be ~1.3 eV. Thus the vacancy can be expected to be immobile at room temperature on the time scale of NC-AFM frame imaging, e.g., 1 s. Its motion should then be tip-induced or tip-assisted and can be modeled within a static model, using molecular mechanics rather than dynamics. To investigate the effect of tip interaction on the vacancy diffusion barrier, we initially place a Mg-terminated tip at the midpoint of the O diffusion path [see Fig. 5(a)]. It is found that this is a global energy minimum for the oxygen atom when the tip is located at height of 2.5–3.5 Å above the ideal surface, i.e., the energy barrier to diffusion is completely removed. This suggests that "assistance" provided by the tip in this case concerns the *reduction of a vacancy diffusion barrier* by the tip electrostatic potential, shown in Fig. 6,

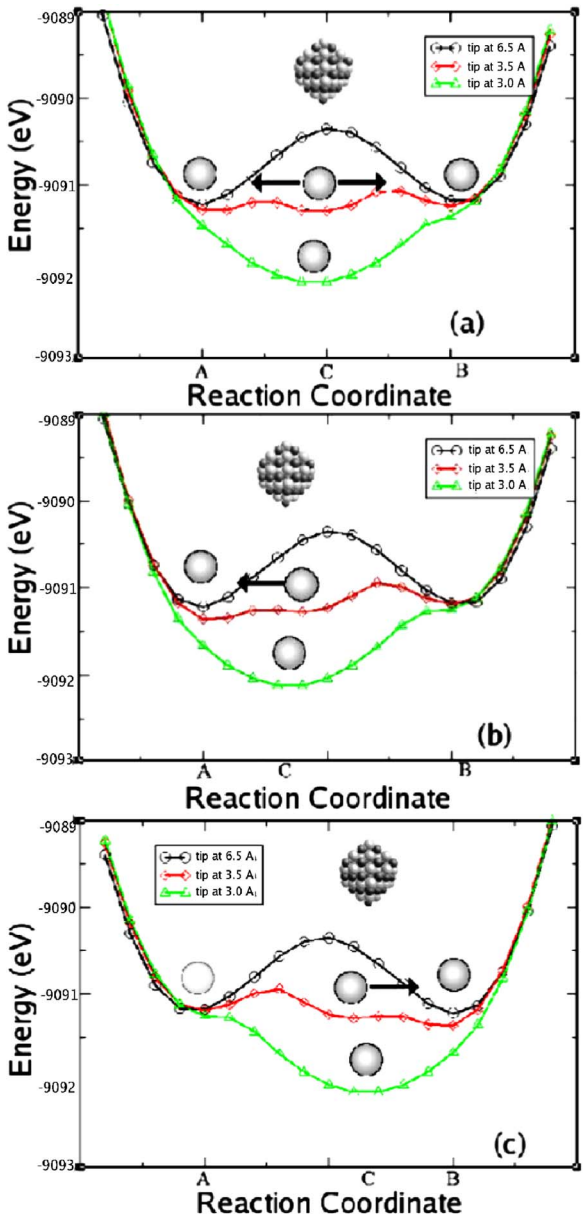

FIG. 5. (Color online) PES for the tip-induced diffusion of a vacancy on a MgO(001) surface. The reaction coordinate corresponds to the motion of an oxygen atom neighboring the vacancy in a (110) direction to occupy the vacancy site. The oxygen atom is initially located at point *A*, and the vacancy at point *B*. *C* indicates the position of the tip. In particular, (a), (b), and (c) show the PES evolution with the tip at a point almost equidistant from *A* and *B*, located nearer to *A* and closer to *B*, respectively.

which should facilitate *thermal* vacancy diffusion. Figure 6 also shows the localized character of the potential gradient induced by the tip—the field gradient exceeds 1.0 V/Å directly under the tip at vertical distances less than 3 Å. At the same vertical distance, the field gradient drops below 0.5 V/Å at lateral distances of 1.5 Å. This manipulation mode differs from those considered in the previous section in that the tip does not cause the ion displacement by direct application of a force but rather guides and facilitates the thermal diffusion process. We will discuss the mechanism of

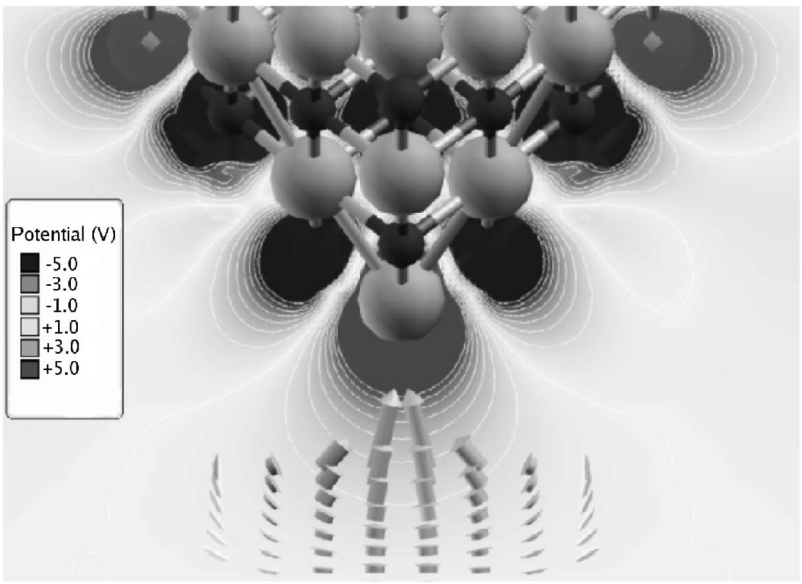

FIG. 6. Electrostatic potential and potential gradient of a Mg-terminated MgO nanotip. Isolines for the potential are spaced 1 V apart. The arrows show the field gradient on a grid with mesh 1.0×1.0 Å. The points nearest the Mg tip are 3.0 Å vertically displaced from the tip apex and show a field gradient of 1.15 V/Å.

this process and its implications for a real dynamic tip in the next section. Using the same parameters as described in Sec. III, the lowering of the tip to 3.0–3.5 Å corresponds in our simulation to an increase in frequency detuning of cantilever oscillations, *df*, to, on average, 220 Hz at 3.5 Å and 340 Hz at 3.0 Å.

B. Mechanism of manipulation

Although our calculations are done statically, it is possible to see qualitatively what would occur in real experimental conditions with the tip oscillating near the cantilever's resonance frequency. As shown in Fig. 5, the potential energy for an O ion depends on the tip location and height. We consider the motion of an O atom initially located at point *A* into the neighboring vacancy, point *B*, through the medium position between the two O sites, point *C*. Figure 5 corresponds to three different tip positions. In this simple case, we can define a reaction coordinate for the diffusion of the vacancy as the motion of the O atom between *A* and *B* along a (110) crystal axis and construct the adiabatic potential energy surface (PES) for the motion of an O ion into the vacancy at different tip positions using a constrained minimization scheme. In these calculations, the O ion is held fixed at some position along the reaction coordinate and all other ions in the region 1 of the surface and the tip (see Fig. 1) are allowed to relax.

If the NC-AFM operates such that the tip apex does not approach nearer than ~4 Å to the surface, there is a height-dependent barrier to motion of the O atom between points *A* and *B* and the PES is of a double-well form—with the tip located at infinity we have an isolated surface defect and a barrier height for vacancy diffusion of 1.3 eV. If the tip is allowed to approach closer to the surface, an additional potential well for the O atom under the tip apex is created, resulting in a triple-well structure. This has the effect of reducing the barrier height for vacancy diffusion. If the tip is allowed to approach even closer, the PES changes such that there is a single stable location for the O atom directly under the tip apex. Upon tip retraction, these changes in the PES are reversed—the stable location under the tip becomes unstable and the O ion can move back to a lattice site, either position *A* where is was initially located, or position *B*, which implies tip-induced diffusion of the vacancy.

The presence of the tip facilitates the motion of the O atom by allowing it to move more freely in the *z* direction, perpendicular to the surface. Without the tip, the O ion cannot move far above the surface plane without a prohibitive loss of Madelung energy, and consequently must force two Mg ions apart during the diffusion motion, with a consequent energy cost. The tip alleviates this by providing an additional, stabilizing, electrostatic field that allows the O atom to move above the surface. Figure 7 demonstrates that, as the tip approaches, the O ion moves over the bottleneck caused by the Mg ions, the O ion being 1 Å above the ideal surface

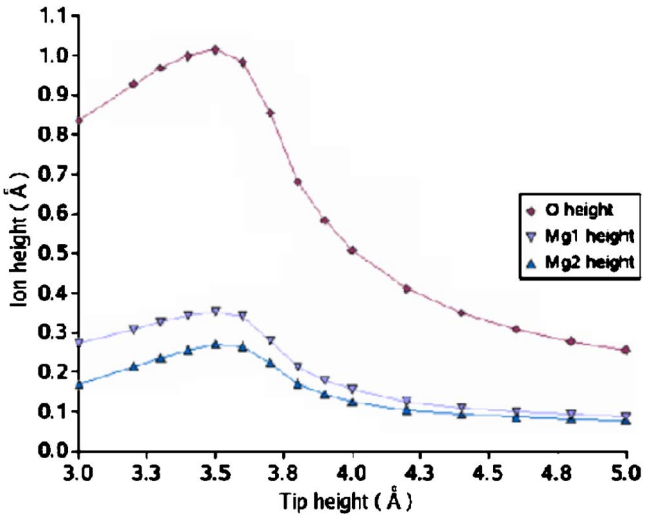

FIG. 7. (Color online) Maximum vertical displacement of the moving O ion and neighboring Mg ions along the reaction path during manipulation as a function of tip height. The tip is located at the position shown in Fig. 5(b).

when the tip approaches to 3.5 Å. The O ion is also followed by the Mg ions to stabilize the O ion through its motion (Fig. 7). We note that the tip does not significantly change the motion of the Mg ions parallel to the surface, and, thus, the action of the tip is to allow the O ion freedom in the z direction, rather than to force the surface Mg ions apart.

If the tip is not located equidistant from points A and B, the energy barriers for the O ion to move into the wells centered at A and B will be different, and the O ion will accordingly be statistically located at one of the lattice sites depending upon the relative sizes of the energy barriers. This is caused by the rapid decrease in electrostatic potential away from the tip apex, with the field gradient varying significantly over the distance 3.13 Å that separates the two O ion lattice sites (see Fig. 6). Figures 5(a)–5(c) show the PES evolution with the tip at a point almost equidistant from A and B (the transition state for non-tip-assisted diffusion), located nearer to A and closer to B, respectively. It can be seen from Figs. 5(b) and 5(c) that the tip breaks the symmetry of the PES, with energy barriers being reduced preferentially near the tip. This means that as the tip approaches, the O atom becomes increasingly likely to occupy the O site below. Upon retraction of the tip, the energy barrier to move into the site further from the tip is significantly larger than to the nearer site at all tip distances until the original double-well structure, and consequent thermal stability of the O ion, is restored. Hence, controlled manipulation occurs. This mechanism also allows us to predict the motion of the O vacancy and how it will depend on scan direction.

We note that this picture of the manipulation process implies that there is unlikely to be a single manipulation event, rather the O atom will jump statistically between the surface sites depending on the tip location and the evolution of the PES during tip oscillation. We also considered manipulating the vacancy using a repulsive O-terminated tip. We found, however, that manipulation in this mode is harder to achieve. We intend to examine this mechanism on a softer substrate.

C. Dependence of manipulation on AFM experimental setup

The manipulation of an O vacancy will depend on several parameters of experiment, such as the nearest approach of the tip to the surface and the amplitude of the tip oscillations. These parameters determine the evolution of the PES during the manipulation event. The distance of nearest approach must be such that the tip is close enough to the surface to allow the O ion to move in the z direction to significantly lower or completely remove the barrier for vacancy diffusion. The amplitude of oscillation would ideally be set so as to optimize the time in which the tip is within the manipulation regime.

In addition, different strategies could be used to control the direction of manipulation. One such strategy could involve initial imaging of the defect and then positioning the tip directly above the specific sites where it will facilitate the ion transfer [see, for example, Fig. 5(c)]. In this case, one should rely on an extremely precise tip positioning system and be sure of the positive outcome of the tip-surface interaction. Fingerprints of successful manipulation in terms of topographic and dissipation signals will be discussed elsewhere.

This mode is not the only one that offers the possibility of a continuous movement of the vacancy. In particular, if the tip is moved in a (110) direction and switched from an imaging to manipulation height for a forward scan and back to the imaging height for the backward scan, this could facilitate continuous controlled manipulation along the (110) direction (see Fig. 4). However, in this mode it would be difficult to move the vacancy in any other direction. Such a possibility is offered by scanning along (100) as a fast scan direction (see Fig. 4). In this case, however, the control over the precise direction of manipulation may prove to be weaker as both ions 1 and 2 in Fig. 4 could jump into the vacancy when the tip is located at any position beyond the point **X** in Fig. 4.

These manipulation strategies would require control software beyond, or at limits of, that currently available. However, developments in software are having an impact on the capabilities of AFM, for example,[39] and should continue to develop rapidly.

V. DISCUSSION

We have examined prototypical defects on the surface of a generic oxide, MgO, and studied possible mechanisms of their manipulation with NC-AFM. We first discussed possible methods to characterize the nanotip of the AFM. With NC-AFM, the exact nature of the tip is more important than in the case of STM as only short-range chemical forces are involved in image contrast formation and manipulation of surface species. To this end, we simulated NC-AFM images of a Ca substitutional defect on the MgO surface aiming to help identify a site where tip polarity could be reliably identified, and also presenting a possible target for manipulation. Ca is always present in MgO samples in appreciable concentrations and can be easily doped, if necessary. We do not, however, argue that this is the only candidate. OH groups formed by the reaction of the surface with nascent H_2O, which is always present in sample chambers, are another possibility. We will discuss this in more detail elsewhere. The main point we would like to make is that if one is interested in using a particular surface as a playground for studying surface processes, intentional use of specific dopants could be beneficial for tip characterization. Similar impurities are always present in other systems [e.g., Cr in Al_2O_3 (Ref. 40)].

We also note that while imaging with either tip polarity, the Ca defect appears significantly larger than its true size covering neighboring lattice sites. Given that the Ca substitutional defect causes a very modest change to the surface, this indicates that care must be taken in interpretation of experimental images—a charged defect would probably produce an even larger image and could be mistaken for an aggregate or multicenter defect.

We demonstrated that for oxides with high ionic charges, substitutional defects are not amenable to manipulation, but that the polar tip can exert a strong influence on the barrier to

exchange the defect with neighboring ions. We found that operating in a repulsive manipulation mode was difficult on MgO. The problem here is as much geometric as presenting any inherent objection to pushing—the flat surface of MgO makes applying repulsive lateral forces to the defects difficult, and marked changes to the tip and/or surface limit the repulsive force that can be applied. This highlights the need for effective tip characterization for successful manipulation. We have, however, shown that large changes to diffusion barriers can be exerted by an AFM tip before tip or surface damage and repulsive mode manipulation should certainly be feasible in more favorable systems.

When considering a surface O vacancy, "assistance" provided by the tip may concern the *reduction of a diffusion barrier* by the tip electrostatic potential, which should facilitate *thermal* vacancy diffusion. This differs from the manipulation modes considered for the Ca ion in that the tip does not cause the ion displacement by direct application of a force but rather guides and facilitates the thermal diffusion process. We demonstrated that an oxygen vacancy can easily be moved by this mechanism in a controlled way. To investigate the sensitivity of this result to the exact system considered, we carried out similar calculations using the same nanotip, but on a CaO surface that has a significantly larger lattice constant. Qualitatively the results were the same, but the PES evolved more quickly due to the CaO surface being softer than MgO. The presented model for the vacancy manipulation mechanism is likely to be valid also for simple adsorbed species, such as Cu ions on MgO.[41] Initially, with the tip at a large distance, the PES for such systems appears as the familiar double-well potential. As the tip descends, it must remove the barrier to motion between the wells by either an attractive interaction, as we have illustrated for the O vacancy, or destabilizing the initial position of the target and perhaps stabilizing the position after motion for manipulation in a repulsive mode. As the tip retracts, there must remain an energy barrier to the reverse motion, otherwise the position of the target will be essentially random rather than fully controlled. Further, these conditions will have to hold throughout the scan path to result in successful manipulation. We note that similar issues have recently been discussed in Ref. 42 on the example of single-atom manipulation.

Another benefit of examining these prototype systems is that we can gain insights into the energetic ranges that will lead to successful manipulation. Several clear criteria emerge: the target must be stable on the time scales considered; this means that its barrier to diffusion should be of the order 0.5 eV. While pushing a Ca ion, we managed a reduction in barrier height of $\sim$4.0 eV; this is probably a limiting value for the size of interaction that is achievable. For the oxygen vacancy in an attractive mode, the barrier was reduced from 1.3 eV to actually being a global energy minimum by $\sim$1.0 eV, suggesting that manipulation of barriers up to $\sim$2.5 eV in an attractive mode is feasible. Of course these numbers are dependent on the tip model assumed and the type of surface, but we might expect these numbers to scale roughly as the product of charges for ionic systems. In the case of semiconductor surfaces,[4] manipulation of a process with a typical energy barrier of 0.88 eV was demonstrated, which appears to be in reasonable agreement.

ACKNOWLEDGMENTS

M.W. is funded by EU FP6 project Nanoman. We are grateful to O. Custance, A. Foster, A. Gal, R. Perez, and T. Trevethan for useful discussions.

[1] D. M. Eigler, C. P. Lutz, and W. E. Rudge, Nature (London) **352**, 600 (1991).
[2] J. K. Gimzewski and C. Joachim, Science **283**, 1683 (1999).
[3] S. W. Hla and K. H. Rieder, Annu. Rev. Phys. Chem. **54**, 307 (2003).
[4] S. Morita, I. Yi, Y. Sugimoto, N. Oyabu, R. Nishi, O. Custance, and M. Abe, Appl. Surf. Sci. **241**, 2 (2005).
[5] S. Morita, Y. Sugimoto, N. Oyabu, R. Nishi, O. Custance, Y. Sugawara, and M. Abe, J. Electron Microsc. **53**, 163 (2004).
[6] N. Oyabu, O. Custance, I. S. Yi, Y. Sugawara, and S. Morita, Phys. Rev. Lett. **90**, 176102 (2003).
[7] N. Oyabu, Y. Sugimoto, M. Abe, O. Custance, and S. Morita, Nanotechnology **16**, S112 (2005).
[8] P. Dieška, I. Štich, and R. Pérez, Phys. Rev. Lett. **95**, 111301 (2005).
[9] M. L. Sushko, A. Y. Gal, M. B. Watkins, and A. L. Shluger, Nanotechnology **17**, 2062 (2006).
[10] C. Barth and C. R. Henry, Phys. Rev. Lett. **91**, 196102 (2003).
[11] M. Heyde, M. Sterrer, H. P. Rust, and H.-J. Freund, Appl. Phys. Lett. **87**, 083104 (2005).
[12] S. Hirth, F. Ostendorf, and M. Reichling, Nanotechnology **17**, S148 (2006).
[13] A. L. Shluger, A. L. Rohl, D. H. Gay, and R. T. Williams, J. Phys.: Condens. Matter **6**, 1825 (1994).
[14] A. I. Livshits, A. L. Shluger, A. L. Rohl, and A. S. Foster, Phys. Rev. B **59**, 2436 (1999).
[15] A. S. Foster, A. Y. Gal, J. D. Gale, Y. J. Lee, R. M. Nieminen, and A. L. Shluger, Phys. Rev. Lett. **92**, 036101 (2004).
[16] L. N. Kantorovich, A. L. Shluger, and A. M. Stoneham, Phys. Rev. B **63**, 184111 (2001).
[17] A. S. Foster, C. Barth, A. L. Shluger, R. M. Nieminen, and M. Reichling, Phys. Rev. B **66**, 235417 (2002).
[18] A. S. Foster, C. Barth, A. L. Shluger, and M. Reichling, Phys. Rev. Lett. **86**, 2373 (2001).
[19] K. Fukui, S. Takakusagi, R. Tero, M. Aizawa, Y. Namai, and Y. Iwasawa, Phys. Chem. Chem. Phys. **5**, 5349 (2003).
[20] W. A. Hofer, A. S. Foster, and A. L. Shluger, Rev. Mod. Phys. **75**, 1287 (2003).
[21] F. J. Giessibl, Rev. Mod. Phys. **75**, 949 (2003).
[22] T. R. Albrecht, P. Grütter, D. Horne, and D. Rugar, J. Appl. Phys. **69**, 668 (1991).
[23] *Non-contact Atomic Force Microscopy*, edited by S. Morita, R. Wiesendanger, and E. Meyer (Springer, Berlin, 2002).
[24] F. J. Giessibl, in *Non-contact Atomic Force Microscopy*, edited by S. Morita, R. Wiesendanger, and E. Meyer (Springer, Berlin, 2002), p. 11.

[25] C. Barth, A. S. Foster, M. Reichling, and A. L. Shluger, J. Phys.: Condens. Matter **13**, 2061 (2001).
[26] R. Garcia and R. Perez, Surf. Sci. Rep. **47**, 197 (2002).
[27] A. S. Foster, A. L. Shluger, and R. M. Nieminen, Nanotechnology **15**, S60 (2004).
[28] J. D. Gale, J. Chem. Soc., Faraday Trans. **93**, 629 (1997).
[29] J. D. Gale and A. L. Rohl, Mol. Simul. **29**, 291 (2003).
[30] B. G. Dick and A. W. Overhauser, Phys. Rev. **112**, 90 (1958).
[31] G. Henkelman, B. P. Uberuaga, D. J. Harris, J. H. Harding, and N. L. Allan, Phys. Rev. B **72**, 115437 (2005).
[32] E. A. Colbourn, W. C. Mackrodt, and P. W. Tasker, J. Mater. Sci. **18**, 1917 (1983).
[33] F. Papillon, P. Wynblatt, and G. S. Rohrer, Recrystallization and Grain Growth Pts. 1 and 2 **467**, 789 (2004).
[34] Y. Yan, M. F. Chisholm, G. Duscher, A. Maiti, S. J. Pennycook, and S. T. Pantelides, Phys. Rev. Lett. **81**, 3675 (1998).
[35] E. S. Hellman and E. H. Hartford, Appl. Phys. Lett. **64**, 1341 (1994).
[36] Y. F. Yan, M. F. Chisholm, S. J. Pennycook, and S. T. Pantelides, Surf. Sci. **442**, 251 (1999).
[37] R. Bennewitz, S. Schar, E. Gnecco, O. Pfeiffer, M. Bammerlin, and E. Meyer, Appl. Phys. A **78**, 837 (2004).
[38] O. Custance, R. Nishi, and S. Morita (private communication).
[39] M. Abe, Y. Sugimoto, O. Custance, and S. Morita, Appl. Phys. Lett. **87**, 173503 (2005).
[40] E. Gaudry, D. Cabaret, P. Sainctavit, C. Brouder, F. Mauri, J. Goulon, and A. Rogalev, J. Phys.: Condens. Matter **17**, 5467 (2005).
[41] N. Lopez, F. Illas, N. Rösch, and G. Pacchioni, J. Chem. Phys. **110**, 4873 (1999).
[42] L. Pizzagalli and A. Baratoff, Phys. Rev. B, **68**, 115427 (2003).